Acta Neuropathol
DOI 10.1007/s00401-012-0951-2

ORIGINAL PAPER

Joubert syndrome: brain and spinal cord malformations in genotyped cases and implications for neurodevelopmental functions of primary cilia

Gordana Juric-Sekhar · Jonathan Adkins · Dan Doherty · Robert F. Hevner

Received: 19 January 2012 / Revised: 25 January 2012 / Accepted: 27 January 2012

Abstract Joubert syndrome (JS) is an autosomal recessive ciliopathy characterized by hypotonia, ataxia, abnormal eye movements, and intellectual disability. The brain is malformed, with severe vermian hypoplasia, fourth ventriculomegaly, and "molar tooth" appearance of the cerebral and superior cerebellar peduncles visible as consistent features on neuroimaging. Neuropathological studies, though few, suggest that several other brain and spinal cord structures, such as the dorsal cervicomedullary junction, may also be affected in at least some patients. Genetically, JS is heterogeneous, with mutations in 13 genes accounting for approximately 50% of patients. Here, we compare neuropathologic findings in five subjects with JS, including four with defined mutations in *OFD1* (2 siblings), *RPGRIP1L*, or *TCTN2*. Characteristic findings in all JS genotypes included vermian hypoplasia, fragmented dentate and spinal trigeminal nuclei, hypoplastic pontine and inferior olivary nuclei, and nondecussation of corticospinal tracts. Other common findings, seen in multiple genotypes but not all subjects, were dorsal cervicomedullary heterotopia, nondecussation of superior cerebellar peduncles, enlarged arcuate nuclei, hypoplastic reticular formation, hypoplastic medial lemnisci, and dorsal spinal cord disorganization. Thus, while JS exhibits significant neuropathologic as well as genetic heterogeneity, no genotype–phenotype correlations are apparent as yet. Our findings suggest that primary cilia are important for neural patterning, progenitor proliferation, cell migration, and axon guidance in the developing human brain and spinal cord.

Keywords Joubert syndrome · Ciliopathy · Cerebellar malformation · Vermis aplasia · Brainstem malformation · Spinal cord malformation

G. Juric-Sekhar · R. F. Hevner (✉)
Department of Neurological Surgery,
Seattle Children's Research Institute, University of Washington,
Box C9S-10, 1900 Ninth Ave, Seattle, WA 98101, USA
e-mail: rhevner@uw.edu

J. Adkins · D. Doherty (✉)
Department of Pediatrics, Seattle Children's Research Institute,
University of Washington, Seattle, WA, USA
e-mail: ddoher@uw.edu

Introduction

Joubert syndrome (JS) is a rare genetic neurodevelopmental disorder, first described in 1969 [33], in which specific breathing and movement abnormalities are associated with cerebellar vermis aplasia/hypoplasia and other brain and spinal malformations. Affected patients manifest early hypotonia followed by ataxia, episodic apnea and/or hyperpnea, abnormal eye movements, developmental delay, and intellectual disability. In addition, retinal dystrophy, hepatic fibrosis, cystic kidneys, endocrine abnormalities, encephalocele and polydactyly are seen in some patients [5, 8, 16, 32, 33, 35, 45, 63]. The "molar tooth" sign (MTS) on axial magnetic resonance imaging (MRI) is key to the diagnosis of JS [39, 40, 43, 44, 49, 50, 52, 60]. The molar tooth appearance arises from an enlarged fourth ventricle, deep interpeduncular fossa, and nondecussated/elongated and horizontally oriented superior cerebellar peduncles. Other central nervous system (CNS) abnormalities described in association with JS include nondecussation of the corticospinal tracts and aplasia or hypoplasia of cerebellar and brainstem nuclei [7, 23, 32, 39, 64, 67, 69]. Genetic studies have shown that JS belongs to the class of disorders known as ciliopathies, in which biological functions of the primary

Published online: 14 February 2012

cilium, a nonmotile organelle found on many cell types, are disturbed [55, 57]. Examples of some other ciliopathies include forms of polycystic kidney disease, retinitis pigmentosa, Bardet–Biedl syndrome, and Meckel syndrome.

An autosomal recessive disorder, JS is nevertheless genetically heterogeneous, with at least 13 causative genes identified to date: *NPHP1*, *AHI1*, *CEP290*, *RPGRIP1L*, *MKS3/TMEM67*, *CC2D2A*, *ARL13B*, *INPP5E*, *TMEM216*, *OFD1*, *KIF7*, *TCTN1* and *TCTN2* [5, 12, 16, 18, 24, 26, 45, 49, 55]. However, these known genes account for only <50% of patients [16], and it is likely that additional JS genes will be discovered. Moreover, genetic studies have revealed that JS is allelic with Meckel syndrome (MKS), a lethal disorder characterized by posterior fossa brain malformation (usually encephalocele), cystic kidney disease, congenital liver fibrosis and polydactyly. Different mutations in at least six genes can cause JS and MKS. The prevalence of JS has not been precisely determined; it may range between 1 in 80,000 and 1 in 100,000 live births [8, 45]. JS is uniformly associated with developmental disability, and lifespan is usually decreased due to apnea, renal failure, liver fibrosis and other complications [56].

To date, brief reports of neuropathologic findings have been published for patients affected with JS [4, 7, 8, 25, 31–33, 64, 67], but detailed neuropathology observations have been described in only three patients [23, 64, 67]. Therefore, the spectrum of gross and microscopic abnormalities has remained incompletely defined in JS. And, in light of the documented genetic heterogeneity, the possibility of genotype–phenotype correlations remains to be explored. Here, we describe neuropathological findings in five subjects with JS. These abnormalities provide clues to the underlying developmental mechanisms causing the brain malformations seen in JS.

Materials and methods

Study subjects

Five subjects with JS (four males and one female) from four families were included in the study (Table 1), which was conducted at Seattle Children's Hospital and the University of Washington, Seattle, WA, USA, with approval of the Institutional Review Board. The following inclusion criteria were used: (1) postnatal diagnosis (Subjects 4–5): the "molar tooth sign" characterized by cerebellar vermis hypoplasia and thick, horizontally oriented superior cerebellar peduncles; (2) prenatal diagnosis (Subjects 1–3): The molar tooth sign is not consistently reported in fetuses before 24 weeks [17, 22, 53, 54]; therefore, vermis hypoplasia and elevated roof of the fourth ventricle were used for the prenatal diagnosis of JS.

Subject 1

Maternal history of a prior child with JS prompted close monitoring of this pregnancy. The pregnancy and family history were otherwise unremarkable.

Subjects 2 and 3

The parents of consecutive male fetuses were both healthy, and the family history was unremarkable, but recurrence in male siblings raised concern for autosomal recessive or X-linked inheritance.

Subject 4

After an unremarkable pregnancy, this male subject presented as a neonate with hypotonia and apnea. Electroencephalograms were consistent with diffuse encephalopathy. He did not have kidney, liver or other medical problems. At 13 months of age, the child was found face down and unresponsive in his crib after having breathing difficulties overnight.

Subject 5

This girl was exposed to alcohol and cocaine in utero, and had poor prenatal care. Family history was significant for consanguinity and mental health problems. She developed intestinal pseudo-obstruction syndrome and bacterial overgrowth involving the small intestine, eventually requiring parenteral nutrition and multiple intestinal surgeries. At 22 years of age, she developed septic shock secondary to a central line infection with *Klebsiella pneumoniae*, *Staphylococcus* sp. and *Candida tropicalis*.

Imaging studies

Fetal subjects [1–3] were imaged by ultrasound prior to MRI in 3 planes using single-shot fast spin echo (FSE) sequences after 20 weeks gestation. The postnatal Subjects 4 and 5 had at least the following brain MR sequences: axial and coronal T1, axial and coronal T2 or FLAIR-weighted images. Slice thickness ranged from 4 to 5 mm with 0–2 mm between slices.

Genetic testing

The subjects were evaluated for the common *NPHP1* deletion by microsatellite genotyping [30], and/or sequenced for one or more of ten genes known to be responsible for Joubert syndrome [16]. Forward and reverse strands of all exons plus 30–50 base pairs of flanking intronic DNA were sequenced as described previously [18]. When parental and/or sibling

Table 1 Clinical features in five subjects with Joubert syndrome

Subject no.	1	2	3	4	5
Mutation	*RPGRIP1L* c.1897T>C, p.C633R c.2582InsT, p.L861LfsX6	*OFD1* c.277G>T, p.V93F	*OFD1* c.277G>T, p.V93F	*TCTN2* c.1117G>A, p.G373R c.76delG, p.D26TfsX26	Unknown
Sex	M	M	M	M	F
Age at death	22.3 wg	22 wg	20.6 wg	13 months	22 years
Ethnic origin	Caucasian	Caucasian	Caucasian	Caucasian	Caucasian
Consanguinity	No	No	No	No	Yes
Affected siblings	1 F	1 M	1 M	No	No
Unaffected siblings	2 F	No	No	2 F	6 half-siblings
Pregnancy/birth weight	TP	TP	TP	40 wg; 3.84 kg	Term
Cephalocele	No	Yes	Yes	No	No
Cleft soft palate	No	Yes	No	Yes	No
Retinal dystrophy	NA	NA	NA	No	No
Coloboma	NA	NA	NA	No	No
Cystic kidney disease	No	No	No	No	Yes
Congenital hepatic fibrosis	No	Yes	Yes	No	No
Polydactyly	No	Post-axial	No	No	No
Episodic hyperpnea/apnea				Yes	NA
Vision impairment				Yes	Yes
Hearing impairment				No	Yes
Hypotonia				Yes	Yes
Developmental delay				Yes	Yes
Other features				Tongue protrusion; torticollis without cervical vertebral abnormalities; dysphagia GERD	Scoliosis; attention deficit disorder; seizures; RTA type IV; sleep apnea; long QT syndrome; intestinal pseudo- obstruction syndrome
Cause of death				Presumed respiratory failure	Septic shock

M male, *F* female, *wg* weeks gestation, *NA* not available, *TP* termination of pregnancy, *GERD* gastroesophageal reflux disease, *RTA* renal tubular acidosis

DNA was available, we evaluated whether the mutations segregated appropriately for the mechanism of inheritance (X-linked for *OFD1* and autosomal recessive for all other genes). The PolyPhen-2 [48] and SIFT prediction programs were used to determine the likelihood that the missense mutations are deleterious, and the frequency of mutations in European American subjects without severe congenital disorders was examined using data available through the NHLBI Exome Sequencing Project [20].

Tissue preparation and immunohistochemistry

Autopsy specimens of brain and spinal cord were fixed in 10% buffered formalin and embedded in paraffin. Sections were routinely stained with hematoxylin and eosin (HE). The following primary antibodies were used for immunohistochemistry: monoclonal mouse anti-neurofilament (NF) protein (1:400; DAKO, Carpinteria, CA, USA), polyclonal rabbit anti-calretinin (1:1,000; Cell Marque, Rocklin, CA, USA), monoclonal mouse anti-microtubule-associated protein 2 (MAP2) (1:1,000; Millipore, Billerica, MO, USA), monoclonal mouse anti-synaptophysin (1:800; BioGenex Laboratories, San Ramon, CA, USA), monoclonal mouse anti-myelin basic protein (MBP) (1:20; Millipore, Billerica, MO), and monoclonal mouse anti-glial fibrillary acidic protein (GFAP) (DAKO, Carpinteria, CA, USA).

Structures diagnosed as abnormal in affected specimens were compared with age-matched control specimens (without brain or spinal malformations) from archival autopsy materials in the Department of Pathology at Seattle Children's Hospital, Seattle, WA.

Results

Neuroradiology findings

All subjects displayed the core imaging features of JS, including vermis hypoplasia and thick, horizontally oriented superior cerebellar peduncles (Fig. 1). Imaging features of Subject 1 have been reported previously [15]. The MTS was demonstrated on postnatal imaging in Subject 4 (Fig. 1d) and Subject 5 (Fig. 1f); however, while the MTS can be identified in some fetuses before 22 weeks gestation [17, 22, 53, 54], it was not demonstrated on axial views of fetal MRIs in Subjects 1–3. Additional findings not seen in all patients with JS included: (1) abnormal excess tissue on the dorsal aspect of the cervicomedullary junction in Subjects 2–4; (2) small occipital meningocele in Subjects 2–4; (3) enlarged posterior fossa in Subjects 2 and 3; (4) an abnormally thick and dysplastic tectum in Subject 4; and (5) prominent fluid spaces between the cerebellar folia giving an atrophic appearance in Subject 5.

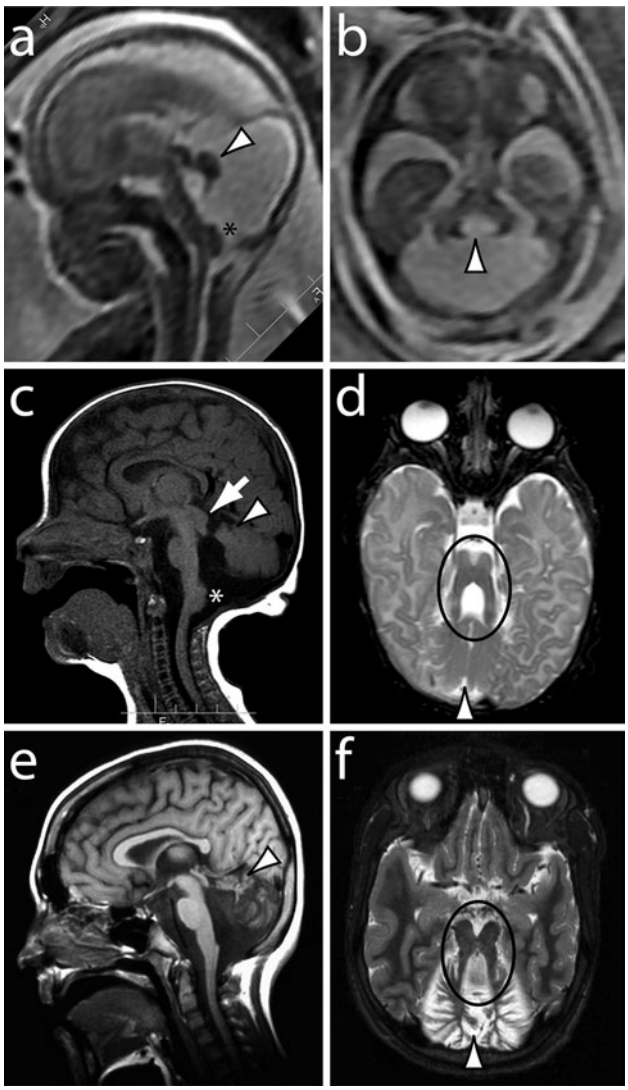

Fig. 1 MRI findings in Subjects 2, 4 and 5. **a**, **b** Subject 2 at 21 wg; **c**, **d** Subject 4 at 5 weeks; **e**, **f** Subject 5 at 13 years. All subjects have vermis hypoplasia (*arrowheads*) on sagittal (**a**, **c**, **e**) and axial (**b**, **d**, **f**) views. The roof of the 4th ventricle is more horizontally oriented than normal, indicating horizontal orientation of the SCPs. The hemispheres impinge on the midline in Subject 4, making it difficult to see the vermis hypoplasia on the sagittal view (*arrowhead* in **c**). The molar tooth sign (long thick superior cerebellar peduncles and deep interpeduncular fossa) is apparent on axial views in Subjects 4 and 5 (*circles* in **d** and **f**, respectively). As expected, thick, horizontally oriented SCPs are not demonstrated on axial views in fetal Subject 2 (**b**), but are apparent in postnatal Subjects 4 (**d**) and 5 (**f**). Abnormal excess tissue is present on the dorsal aspect of the cervicomedullary junction in Subjects 2 and 4 (*asterisks* in **a**, **c**). The posterior fossa is enlarged in Subject 2 (**a**), and Subject 4 has an abnormally thick and dysplastic tectum (*arrow* in **c**). Subject 5 has prominent fluid spaces between the cerebellar folia giving an atrophic appearance (**f**)

Genetic testing

Subject 1 had compound heterozygous mutations in the *RPGRIP1L* gene: a missense change in a highly conserved residue of the first calcium-dependent lipid binding (C2)

Table 2 Macroscopic brain and spinal cord examination in five subjects with Joubert syndrome

Subject no.	1	2	3	4	5
Fixed brain weight (normal mean ± SD)	72.69 g (78.15 ± 14.37 g)	103.0 g (78.15 ± 14.37 g)	70.0 g (55.38 ± 10.18 g)	1,215 g (970.0 ± 53.0 g)	890 g (1,198.0 ± 124.0 g)
Infratentorial weight (normal mean ± SD)	NA	5.4 g (3.71 ± 0.74 g)	4.0 g (2.81 ± 0.42 g)	187.4 g (178.0 ± 24.0 g)	NA
Infratentorial/total brain ratio (normal ratio ± SD)	NA	5.2% (4.54 ± 0.41%)	5.7% (4.98 ± 0.49%)	15.4% (12.91 ± 1.44%)	NA
Meningocele	No	Occipital	Occipital	NA	No
Cerebellum	Hypoplastic	Hypoplastic	Hypoplastic	Distorted hemispheres wrapping anteriorly around the brain stem	Hypoplastic
Vermis	Aplastic	Hypoplastic	Hypoplastic	Aplastic	Aplastic
Dentate nucleus	NA	NA	NA	Hypoplastic/fragmented	Hypoplastic/fragmented
Fourth ventricle	Enlarged	Enlarged	Enlarged	Enlarged	Enlarged
Medulla oblongata	Normal	Dorsal enlargement	Dorsal enlargement	Dorsal enlargement, elongated, small inferior olives	Normal
Pons	Normal	Flat appearance	Normal	Normal	Elongated SCP
Midbrain	Normal	Normal	Normal	Small substantia nigra	Lightly pigmented substantia nigra
Gyral/sulcal pattern	Normal	Normal	Normal	Gyral hyperconvolution in parietal lobes/Sylvian fissure shorter on the R	Atrophic
Coronal sections	Recent IVH	Punctuate periventricular hemorrhage; L recent IVH	Hypoplastic basal ganglia	Slightly hypoplastic uncus and parahippocampal gyri; R hippocampus smaller than L	Normal
Spinal cord	Cervical cord normal	Normal	Normal	NA	Normal

L left, *R* right, *NA* not available, *SCP* superior cerebellar peduncle, *IVH* intraventricular hemorrhage

domain (c.1897T>C, p.C633R), and a single base pair insertion predicted to truncate the protein in the second C2 domain (c.2582InsT, p.L861LfsX6). The missense change is not listed in dbSNP131 and was not identified in 2,700 control chromosomes.

Subjects 2 and 3 had a missense change in the *OFD1* gene (c.277G>T, p.V93F). Amino acid 93 is located within the LisH domain required for OFD1 function and it is conserved throughout the animal kingdom, except in *Tetrahymena*. V93F is also predicted to be deleterious by the modeling programs SIFT and PolyPhen-2 [1], is not listed in dbSNP131 and the change was not identified in 2,696 control chromosomes. OFD1 regulates centriole length [61] and is required for pericentriolar satellite integrity [38]. Missense mutations in the LisH domain disrupt these activities and have been associated with orofaciodigital (OFD) syndrome in female patients [48].

Subject 4 had compound heterozygous mutations in the *TCTN2* gene: a missense change (c.1117G>A, p.G373R) and a single base pair insertion predicted to truncate the protein near the N terminus (c.76_77delG, p.D26TfsX26). TCTN2 has no known functional domains, but has been implicated in Sonic hedgehog (Shh) signaling and recently reported in patients with JS and MKS [53]. The missense change is predicted to be deleterious by PolyPhen-2, is not listed in dbSNP131 and was not identified in 2,654 control chromosomes.

Sequence data were only available for the *TMEM67* and *CC2D2A* genes in Subject 5 and no deleterious variants were identified.

General autopsy findings

Subjects 1–3 displayed gestationally appropriate measurements and normal external and internal features except as follows. Subject 1 showed mild pectus excavatum, telecanthus (inner canthal distance 18.2 mm, >2 SD for gestational age) and a single palmar crease on the right hand. Subject 2 showed posterior meningocele involving the inferior portion of occipital bone and superior cervical vertebrae, cleft secondary palate, flexion contractures of the right wrist and fingers 2–5, left hand with splayed fingers 2 and 3, left foot with polysyndactyly of the fifth and sixth digits, and a broad fifth digit with two nails. Slightly enlarged and tortuous ureters bilaterally were found in Subjects 2 and 3. The histology of the liver in Subjects 2 and 3 demonstrated enlarged tortuous bile ductules in the portal tracts with fibrosis consistent with hepatic biliary dysgenesis, and the renal cortex demonstrated tubules with minimal tubular dilation and no cyst formation.

Subject 4 displayed compatible measurements with the stated age, and gross and microscopic examinations were normal.

Fig. 2 Brain at postmortem examinations in subjects with Joubert syndrome. **a**, **b** Posterior views of the cerebellum and brainstem in Subjects 2 (**a**) and 3 (**b**) show enlarged wide-open 4th ventricle, hypoplastic vermis and markedly hypoplastic cerebellar hemispheres. Abnormal excess tissue is visible on the dorsal aspect of the cervicomedullary junction (*black arrows*). **c** Cerebellum and brainstem in an age-matched unaffected fetus. **d** The cerebellum and brainstem of Subject 2 (midline cut) demonstrate hypoplastic cerebellum (*black asterisk*), flat pons, and abnormal excess tissue on the dorsal aspect of the cervicomedullary junction (*black arrow*). **e** Subject 4 displays an elongated medulla lacking inferior olivary prominences (*black arrowhead*). No obvious pyramidal decussation is seen (*black arrow*). Cerebellar tissue wraps ventrally around the medulla to the pyramids (*black asterisk*). **f** Mid-pons and cerebellum (cut perpendicular to the long axis at the level of cranial nerve V exit) in Subject 4 show aplasia of the cerebellar vermis (*white arrow*) and enlarged 4th ventricle. Crossing fibers are seen in the hypoplastic basis pontis (*black arrowheads*), and fragmented dentate nuclei are seen bilaterally (*red arrowheads*). **g** The dentate nucleus of Subject 5 is also fragmented (*red arrowheads*). **h** The pons and cerebellum (midline cut, medial view) of Subject 5 demonstrate enlarged 4th ventricle, aplastic vermis (*black asterisk*), and hypoplastic cerebellum. *Scale bar* 1 cm (**a**–**h**)

Subject 5 was a small-for-age, well-nourished female with two well-healed abdominal surgical scars and four ostomies. In addition, the peritoneal surfaces had multiple adhesions involving diaphragm, retroperitoneum, small and large bowels. Gross and microscopic examinations demonstrated a right serous pleural effusion, bilateral lung congestion and edema, right middle and lower lobe thromboemboli in small size arteries and pneumonia, ventricular dysplasia of the right heart, liver fibrosis, congestion and mild steatosis, ascites, chronic pancreatitis, focal and periglomerular sclerosis with focal tubular dilation in both kidneys, and thyroid colloid nodules.

Neuropathologic findings: macroscopic

Macroscopic observations are summarized in Table 2. The most common findings were enlarged fourth ventricle and hypoplastic/aplastic cerebellar vermis (all subjects), followed by hypoplasia of the cerebellar hemispheres (all except Subject 4), abnormal excess tissue on the dorsal aspect of the caudal medulla oblongata (Subjects 2–4) (Fig. 2a, b, d, f, h), and fragmented dentate nuclei (Subjects 4, 5) (Fig. 2f, g). In Subject 4, the decussation of the corticospinal tracts and the typical prominences corresponding to the inferior olives were absent. The distorted cerebellar hemispheres wrapped ventrally around the medulla to the pyramids (Fig. 2e). The superior cerebellar peduncles appeared elongated in Subject 5.

Neuropathologic findings: histologic

The histologic findings are summarized in Table 3. Detailed findings are further described according to region of the central nervous system, as follows.

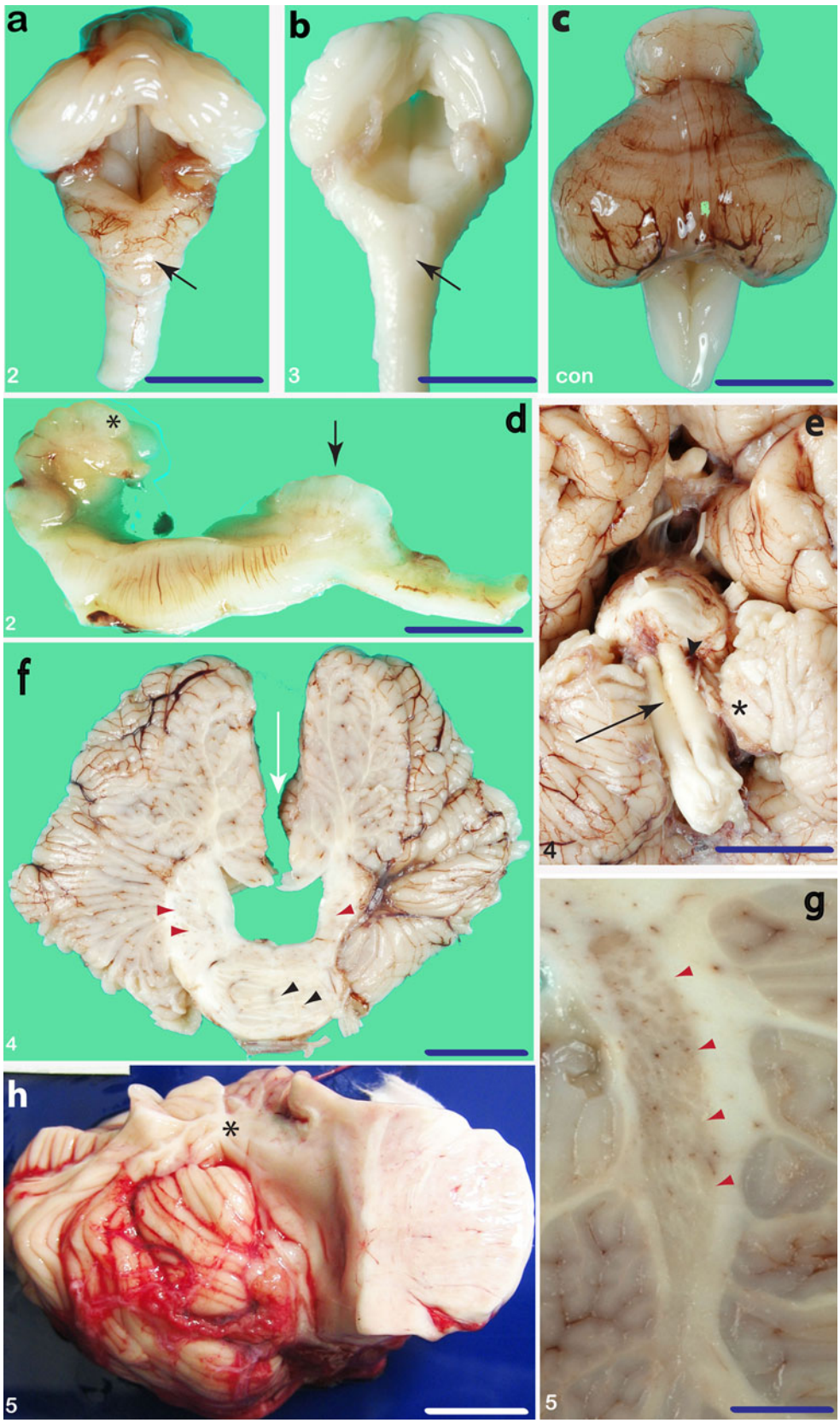
a
2
b
3
c
con
d
*
2
e
*
4
f
4
g
5
h
*
5

Cerebellum

In addition to vermis hypoplasia, we observed fragmentation of the dentate nuclei in all subjects (Fig. 3g). Subjects 2–5 showed reduced numbers of Purkinje cells. GFAP staining revealed either increased (Subjects 4, 5) or decreased (Subjects 1–3) numbers of Bergmann glia (Fig. 3h, i). Subjects 2–5 had cerebellar heterotopia (Fig. 3j).

Brainstem

The pontine nuclei were hypoplastic in all subjects. The inferior olivary nuclei were hypoplastic with simplified convolutions in Subjects 1–4 (Fig. 3d, e), while in Subject 5, the inferior olives demonstrated slightly simplified convolutions with neuronal loss and gliosis, suggesting combined hypoplasia and atrophy. The posterior median sulcus was absent in the lower medulla and upper cervical spinal cord of Subjects 2–4, and was replaced by a heterotopia containing calretinin- and MAP2-positive neurons, GFAP-positive astrocytes, and MBP-positive myelinated axons (Fig. 3a, b). Prominent subpial and periolivary brainstem gliosis were present in Subjects 1–4 (Fig. 3d).

Forebrain

The cerebrum in all subjects showed a well-formed, 6-layered neocortex by HE staining and immunohistochemistry (MAP-2 and calretinin). Normal GFAP-positive radial glia were present in the cerebral cortex of Subjects 1–3. Minute subcortical heterotopia were evident in Subject 4 as well as fragmented claustrum and unlaminated lateral geniculate body.

Spinal cord

The spinal cord, available for examination only in Subjects 2 and 3, revealed dysplastic posterior tracts in the cervical spinal cord and bulky anterior corticospinal tracts (Fig. 3l).

Discussion

Despite increasing clinical recognition of JS and rapid progress in gene identification, few detailed studies of JS neuropathology have been published, and comparisons of brain and spinal cord malformations among different genotypes have been lacking. Our study confirms previous descriptions of malformations in brain and spinal cord of JS patients [4, 7, 8, 23, 25, 31–33, 64, 67, 69], and reveals that some of the phenotypes exhibit incomplete penetrance (summarized in Table 4). Nevertheless, each malformation may be associated with multiple JS genes. Thus, no correlations between JS genotype and neuropathological phenotype can be defined as yet. In addition, we present a novel correlation of brainstem neuroimaging anomalies with dorsal cervicomedullary heterotopia, previously described only by pathology [23, 69] or imaging but not both [46, 47].

Although Subject 5 had the core brain findings seen in patients with JS as well as characteristic cystic kidney disease, she also had small brain size and atrophy, features rarely associated with JS. Therefore, some of the brain abnormalities in this subject may be due to in utero alcohol exposure, chronic severe illness, or may be a manifestation of a particular genetic sub-type of JS not yet described.

JS is a phenotypically and genetically heterogeneous condition. The unifying diagnostic criterion is the molar tooth sign on imaging, and JS patients can have a variety of other features (retinal dystrophy, cystic kidney disease, liver fibrosis, polydactyly, etc.). Despite this phenotypic heterogeneity, the use of the molar tooth sign as the pathognomonic feature of JS has allowed the identification of 13 genes that cause JS over the past 7 years. So far, strong genotype–phenotype correlations have been the exception rather than the rule.

Genetic and phenotypic overlap of JS and related disorders

In the present study, three known JS genes are represented in the five subjects: *OFD1*, *RPGRIP1L* and *TCTN2*. Most commonly, *OFD1* mutations have been described in female patients with OFD type 1, characterized by oral (lobed tongue, tongue hamartomas, abnormal oral frenulae, abnormal palate, alveolar clefts, and/or tooth abnormalities), facial (hypertelorism, nasal hypoplasia, median cleft lip, downslanting palpebral fissures and/or micrognathia) and digital (brachydactyly, syndactyly, and/or polydactyly) malformations [21]. CNS features in these patients often include midline cysts and cortical dysplasia and >50% of patients develop cystic kidney disease. *OFD1* mutations have also been described in male patients with JS [11], as well as male patients with intellectual disability, macrocephaly and motile ciliary dysfunction [6]. While the two male siblings with *OFD1* mutations in our series had oral (cleft soft palate) and digital (post-axial polydactyly) features, they did not have the typical facial features of OFD syndrome [6, 27]. In addition, CNS findings were typical for JS and they also had occipital meningoceles and congenital hepatic fibrosis. Alternatively, the fetuses could be categorized as having MKS, although they lacked the cystic kidney disease that is usually seen in MKS. This distinction may be arbitrary, since JS and MKS are allelic disorders caused by mutations in *MKS3/TMEM67*,

Table 3 Microscopic brain and spinal cord findings in 5 subjects with Joubert syndrome

Subject no.	1	2	3	4	5
Cerebellum					
Dentate nucleus	Fragmented	Fragmented	Fragmented	Fragmented	Fragmented
Cerebellar cortex	Normal	Hypoplastic	Hypoplastic	Normal	Hypoplastic/atrophic
Purkinje cells	Normal	Reduced cellularity	Reduced cellularity	Reduced cellularity	Reduced cellularity
Bergman glia	Reduced	Reduced	Reduced	Increased	Increased
Cerebellar heterotopia	No	Yes	Yes	Yes	Yes
Vermis	Aplasia	Hypoplasia	Hypoplasia	Aplasia	Aplasia
Medulla oblongata					
Decussation of CST	No	NA	Few crossing fibers	Few crossing fibers	NA
Arcuate nucleus	Normal	Hypoplastic	Enlarged	Enlarged	Normal
Inferior olives	Hypoplastic	Hypoplastic	Hypoplastic	Hypoplastic	Reduced cellularity
Spinal nucleus of V	Hypoplastic; fragmented	NA	Fragmented	Fragmented	Fragmented
Reticular formation	Reduced cellularity	NA	Slightly reduced cellularity	Reduced cellularity	Reduced cellularity
Solitary nucleus	Reduced cellularity	Dysplastic	Dysplastic	Dysplastic	Reduced cellularity
Posteromedian sulcus	Yes	No	No	No	Yes
Dorsal dysplastic bulge	No	Yes	Yes	Yes	No
N. gracilis/cuneatus	Normal	Dysplastic	Dysplastic	Dysplastic	Normal
Fasc. gracilis/cuneatus	Normal	Dysplastic	Dysplastic	Dysplastic	Normal
Pons					
Medial lemniscus	NA	Hypoplastic	Hypoplastic	Hypoplastic	Hypoplastic
Trapezoid body	Normal	NA	NA	Normal	Normal
Reticular formation	Reduced cellularity	NA	Reduced cellularity	Reduced cellularity	Reduced cellularity
Pontine nuclei	Reduced cellularity	Reduced cellularity	Reduced cellularity	Reduced cellularity	Reduced cellularity
Midbrain					
Decussation of SCP	Yes	NA	Yes	Hypoplastic	No
Reticular formation	Reduced cellularity	Slightly reduced cellularity	Reduced cellularity	Reduced cellularity	Reduced cellularity
Locus ceruleus	Normal	NA	Normal	Elongated	Elongated
Cerebrum					
Cortical appearance	NL6	Status verrucosus; NL6	Status verrucosus; NL6	NL6	NL6
Subcortical heterotopia	No	No	No	Yes	No
Hippocampus	Normal	Normal	Hypoplastic	Hypoplastic	Normal
Thalamus	Normal	Normal	Disorganized	Reduced cellularity	Normal

Table 3 continued

Subject no.	1	2	3	4	5
Basal ganglia	Normal	Normal	Hypoplastic	Claustrum fragmented	Normal
Lateral geniculate body	Normal	Normal	Normal	Not laminated	Reduced cellularity
Spinal cord					
Cervical	NA	Enlarged anterior funiculi; absent dorsal median sulcus; dysplastic posterior funiculi	Enlarged anterior funiculi; absent dorsal median sulcus; dysplastic posterior funiculi	NA	Normal
Thoracic	NA	Normal	Normal	NA	Normal
Lumbar	NA	Normal	Normal	NA	Normal

NA not available, *CST* corticospinal tract, *SCP* superior cerebellar peduncle, *Cn* cranial nerve, *NL6* normal 6-layered cortex

Fig. 3 Histopathology of the brain and spinal cord. **a** The cerebellum and brainstem of Subject 2 (sagittal section, rostral left) shows dorsal heterotopia with numerous calretinin-positive cells (*black arrow*). The pyramidal tract is appropriately positioned in the brainstem (*black asterisk*). **b**, **c** The medulla of Subjects 1 and 3, immunostained to detect GFAP, shows bilateral periolivary gliosis around the simplified inferior olivary nuclei (*black arrowheads*). **d** The rostral medulla of Subject 4, immunostained to detect NF, demonstrates hypoplastic inferior olivary nuclei (*black arrowheads*), and thickened arcuate nuclei (*black asterisk*). **e** Cervicomedullary junction of Subject 4 immunostained for MBP demonstrates absence of the posterior median sulcus, with disorganized dorsal column tracts and nuclei (*black arrowheads*). Due to nondecussation, the corticospinal tract is located mainly in anterior rather than lateral white matter. A few fascicles of MBP-positive corticospinal fibers cross the midline, as seen at higher magnification in **f** (corresponding to *boxed area* in **e**. **g** The cerebellar cortex in Subject 4 shows an increased GFAP-positive Bergmann glia. **h** GFAP-immunopositivity in the cerebellar cortex from an unaffected age-matched fetus. **i**, **j** The cerebellar cortex in Subjects 1 and 3 shows a paucity of GFAP-positive Bergmann glia, and decreased thickness of external and internal granular layers. **k** The pontomedullary junction in Subject 1 shows vermis aplasia (*HE*). **l** The cerebellar hemisphere of Subject 4 shows fragmented deep nuclei forming a chain of neuronal clusters in the white matter (*NF*). **m** The cervical spinal cord in Subject 2 shows disorganized, poorly defined posterior funiculi with nests of medium-sized neurons (*black arrowheads*), and a poorly formed posterior median sulcus. The anterior corticospinal tracts were greatly enlarged (*black asterisk*), consistent with nondecussation. **n** Axial section of cervical spinal cord from an unaffected age-matched fetus stained with HE. **o** The basal ganglia in Subject 4 demonstrate fragmentation of the claustrum (*black arrows*) with small neuronal heterotopia in the extreme capsule (*MBP*). **p** Cerebellar heterotopia in Subject 5 (stained with HE) consists of disorganized granule cells and Purkinje neurons. *Scale bars* 40 μm (**g**–**i**), 20 μm (**f**, **j**, **p**), 10 μm (**b**–**e**, **l**), 5 μm (**a**, **k**, **m**–**o**). Sections: sagittal (**a**, **l**), axial (**b**–**j**, **m**–**p**), coronal (**o**). *GFAP* glial fibrillary acidic protein, *HE* hematoxylin and eosin, *MBP* myelin basic protein, *NF* neurofilament protein

TMEM216, *RPGRIP1L*, *CEP290*, *CC2D2A*, and *TCTN2* [3, 14, 66] with JS representing the mild end, and MKS the severe end of the spectrum. Of note, *OFD1* mutations have not been described in fetuses with classic MKS. Typically, patients with *RPGRIP1L*-associated JS have progressive renal disease, but not retinal dystrophy, liver fibrosis or polydactyly, and the reported patients with *TCTN2*-associated JS have not had other organ complications.

Despite three distinct genetic causes in Subjects 1–4, the brain abnormalities are quite similar overall. This speaks to the involvement of shared underlying biological mechanisms. All of the genes responsible for JS encode proteins that localize to the cilium and/or basal body. Primary cilia are microtubule-based structures that project from the apical surfaces of most cells. In contrast to motile cilia, primary cilia in general do not have the central two microtubule doublets and are not motile. Primary cilia function to interpret mechanical, chemical and photic signals from the environment and are also required for proper Shh, PDGFα and Wnt signaling [41]. Cilia play a role

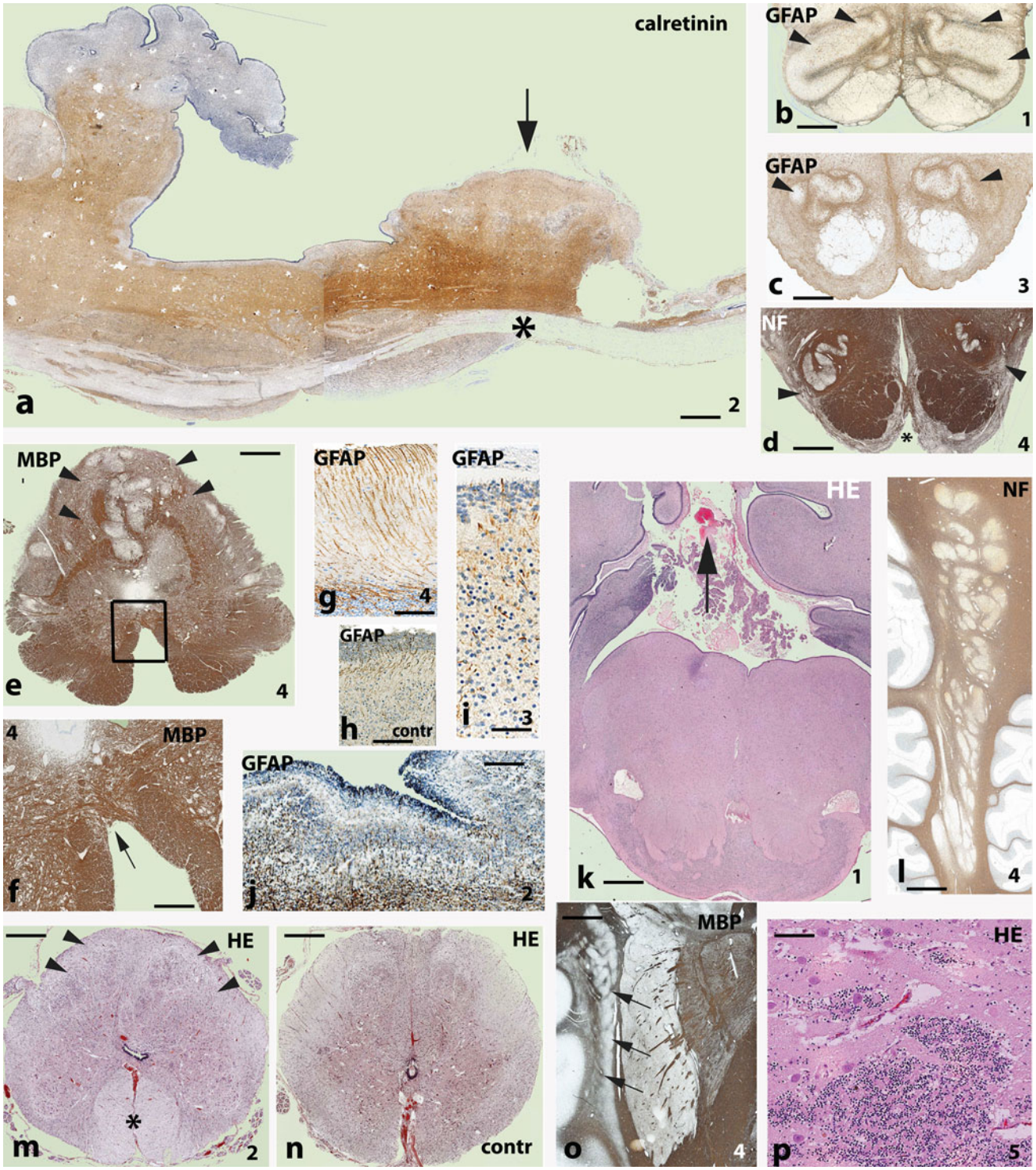

in cerebellar development, as detailed below. Similarly, primary cilia have been implicated in adult neural stem cell maintenance [29], and ependymal cilia are required for migration of some forebrain neurons [58]. Both cilia and the JS genes have been implicated in dorsal–ventral patterning of the neural tube [9, 11, 19, 42]. Cilia have also been implicated in PDGFα-dependent fibroblast migration [59], but direct roles for primary cilia in neuronal migration or axon guidance have not been demonstrated.

The cerebellar malformation in JS

The cerebellar vermis develops and becomes fully foliated by 4 months gestation, while development of the large

Table 4 Neuropathology findings in 13 reported cases with Joubert syndrome with genes associated with structural abnormalities found in present cases

Neuropathology findings	$N = 13$[a,b]	Genotype[c]
Meningocele/encephalocele	5/13	*OFD1*
Vermian aplasia/hypoplasia	13/13	*RPGRIP1L, OFD1, TCTN2*
Fragmented dentate n.	11/13	*RPGRIP1L, OFD1, TCTN2*
Cerebellar heterotopia	9/13	*TCTN2*
Hypoplastic inferior olivary n.	8/12	*RPGRIP1L, OFD1, TCTN2*
Absent decussation of CST	6/9	*RPGRIP1L*
Abnormal arcuate n.	4/5	*OFD1, TCTN2*
Absent posterior median sulcus	4/7	*OFD1, TCTN2*
Disorganized n./fasc. gracilis and cuneatus	6/7	*OFD1, TCTN2*
Absent/hypoplastic solitary n./tract	5/7	*OFD1, TCTN2*
Fragmented spinal n. of V (trigeminal nerve)	6/8	*RPGRIP1L, OFD1, TCTN2*
Hypoplastic reticular formation	6/6	*RPGRIP1L, OFD1, TCTN2*
Hypoplastic pontine n.	6/6	*RPGRIP1L, OFD1, TCTN2*
Absent trapezoid body	3/6	
Absent or poor decussation of SCP	4/7	*TCTN2*
Elongated locus ceruleus	4/7	*TCTN2*
Cortical laminar disorganization	2/7	
Subcortical heterotopia	3/8	*TCTN2*
Abnormal lateral geniculate body	3/6	*TCTN2*
Disorganized dorsal funiculi of CSC	4/5	*OFD1*
Enlarged ventral funiculi of CSC	4/5	*OFD1*

n. nucleus, *fasc*. fasciculus, *CST* corticospinal tract, *SCP* superior cerebellar peduncle, *CSC* cervical spinal cord

[a] Calogero [7], Friede and Boltshauser [23], Giordano et al. [25], Ishikawa et al. [31], Ivarsson et al. [32], ten Donkelaar et al. [64], van Dorp et al. [67], Yachnis [69], present paper

[b] Some malformations were not evaluated in all cases, so the number of cases evaluated for each malformation are indicated as the denominator where appropriate

[c] Genes associated with structural abnormality in present paper

cerebellar hemispheres lags behind that of the vermis by 30–60 days [2]. Hence, the anomaly of the vermis in JS presumably occurs during the early fetal period. In the cerebellum, primary cilia have been identified ultrastructurally in cells of the early rhombic lip, as well as later Purkinje cell and granule cell progenitors [65]. Whereas Shh is expressed in migrating and settled Purkinje cells and stimulates granule cell proliferation [10, 13], it has been hypothesized that the primary defect in JS is compromised granule cell proliferation, resulting in cerebellar hypoplasia [10, 62]. However, this hypothesis does not account for the differential involvement of the vermis, which is absent or severely hypoplastic, as compared to the cerebellar hemispheres, which are not only relatively spared, but also may appear to overgrow the brainstem in some subjects (e.g., Subject 4, Fig. 2e, f). More recent work has implicated the JS gene *AHI1* in Wnt-mediated midline fusion and proliferation of the early cerebellar anlage in mice [36]. An alternative model would involve aberrant dorsal–ventral patterning, as demonstrated in the developing spinal cord of mouse models for *ARL13B*- and *RPGRIP1L*-associated JS [9, 19, 42]. In addition, dysregulation of *GPR56* and other genes that regulate basement membrane integrity also play a role in cerebellar morphogenesis [34].

Aplasia of the cerebellar vermis is one of the crucial malformations that cause MTS, although some proposed JS patients were documented to have normal vermis, isthmus and SCP and were called "JS mimics" [39]. Together, these observations suggest that the cerebellar phenotype in JS arises from a combination of defective patterning (vermis aplasia) and compromised proliferation (overall hypoplasia), along with aberrant cell migration (including fragmentation of the cerebellar nuclei). The attribution of vermis aplasia to defective patterning is consistent with other malformations along the dorsal midline in JS, such as the dorsal cervicomedullary heterotopia, the absent posteromedian sulcus, and spinal posterior column anomalies. In addition, similar cervicomedullary heterotopia has been described in OFD6, although the patients with an OFD6-like presentation have had JS gene mutations; patients

exhibiting such heterotopia without known mutations may have a type of JS that has not yet been genetically characterized [57].

Neurodevelopmental functions of primary cilia implicated in JS

The neuropathological findings in JS indicate derangement of a number of key processes during brain development, including patterning, proliferation, migration, and axon guidance. The abnormalities of SCP decussation found in two of our subjects, and in previously reported JS patients [64, 69], implicate JS genes, and by extension primary cilia, in axon guidance. Likewise, perturbed axon guidance is implicated in pyramidal tract nondecussation, presumably in the early fetal period, since the pyramidal tract has reached the level of the pyramidal decussation at the end of the embryonic period. The numerous heterotopia in several brain regions further implicate primary cilia in neuronal migration [28], a process that involves many of the same cellular and molecular mechanisms as axon guidance. It is tempting to speculate that the spinal cord abnormalities reflect problems with dorsal–ventral patterning, as described in multiple animal models for JS genes (*ARL13B*, *TCTN1*, *TCTN2*, *RPGRIP1L*) [9, 19, 42]. Finally, the vermis hypoplasia and extensive gliosis may indicate defects in neuronal survival, although this could be secondary to defects in cell fate determination, migration or other processes. Anomalies of the solitary tract and gracile nuclei may represent a substrate for the abnormal respiratory pattern, as these centers are known to receive afferent respiratory impulses.

Many questions remain on how JS genetic defects account for the constellation of neuropathologic findings. For example, increased gliosis in the brainstem, cerebellar and cerebral white matter and deep gray nuclei found in our series may suggest reaction caused by either cellular damage or altered fate, or both. The dysplastic abnormalities in the dorsal funiculi of the cervical spinal cord and in the cervicomedullary junction may also reflect disturbances of patterning and cell migration. Although it has been reported that spinal cord patterning is achieved through the coordination of WNT and Shh signaling [51, 70], pathways in which primary cilia play important functions, it is unclear exactly how these processes are disturbed in JS. Interestingly, other CNS abnormalities, such as occipital meningocele (seen in 3 of our 5 subjects; Table 1), have been classified as neurulation defects [68]. Subcortical heterotopia, found in one subject from the present series, is mainly associated with defects in genes that regulate cortical neuron migration including *LIS1*, *TUBA1A*, *TUBB3*, *DCX*, and *FilaminA* [37]. Evidence that JS gene-encoded protein complexes interact with TUBA1A, TUBB3 and FilaminA has been presented [54]. Also among the neuronal migration defects, polymicrogyria has been described in multiple JS patients [15, 31, 47], but such defects might result from environmental as well as genetic insults.

Abnormalities of the CNS found in subjects affected with JS seem to be complex and the developmental mechanisms that generate this complexity have remained elusive. Despite significant advances in the genetics of JS, it is still an enigma how the specific gene defects result in abnormal brain development. According to neuropathology findings, it is reasonable to assume that the brain malformation in JS may be based on abnormal neuronal migration and patterning, aberrant axonal guidance, and gliosis due to cellular death or dysfunction. Further discovery of the molecular basis for CNS abnormalities in JS will aid in diagnosis, genetic counseling, and understanding the role of the JS genes and primary cilia in normal brain development.

Acknowledgments We thank the families of described subjects for giving us permission to study their children. We also thank Drs. Joseph R. Siebert, Raj P. Kapur (Seattle Children's Hospital and University of Washington, Seattle, WA), Robert E. Ruiz (The University of Michigan Hospitals, Ann Arbor, MI), Carol Petito (University of Miami, Miami, Fl), Mason Barr (University of Michigan) and colleagues from the Wayne County Medical Examiner's Office (Romulus, MI) for important assistance to our research. Human tissue was obtained from the NICHD Brain and Tissue bank for Developmental Disorders at the University of Maryland, Baltimore, MD. D.D. was supported by KL2RR025015.

References

1. Adzhubei IA, Schmidt S, Peshkin L, Ramensky VE, Gerasimova A, Bork P, Kondrashov AS, Sunyaev SR (2010) A method and server for predicting damaging missense mutations. Nat Methods 7:248–249
2. Altman NR, Naidich TP, Braffman BH (1992) Posterior fossa malformations. AJNR Am J Neuroradiol 13:691–724
3. Baala L, Romano S, Khaddour R, Saunier S, Smith UM, Audollent S, Ozilou C, Faivre L, Laurent N, Foliguet B, Munnich A, Lyonnet S, Salomon R, Encha-Razavi F, Gubler MC, Boddaert N, de Lonlay P, Johnson CA, Vekemans M, Antignac C, Attie-Bitach T (2007) The Meckel–Gruber syndrome gene, MKS3, is mutated in Joubert syndrome. Am J Hum Genet 80:186–194
4. Boltshauser E, Isler W (1977) Joubert syndrome: episodic hyperpnea, abnormal eye movements, retardation and ataxia, associated with dysplasia of the cerebellar vermis. Neuropadiatrie 8:57–66
5. Brancati F, Dallapiccola B, Valente EM (2010) Joubert syndrome and related disorders. Orphanet J Rare Dis 5:20
6. Budny B, Chen W, Omran H et al (2006) A novel X-linked recessive mental retardation syndrome comprising macrocephaly and ciliary dysfunction is allelic to oral-facial-digital type I syndrome. Hum Genet 120:171–178
7. Calogero JA (1977) Vermian agenesis and unsegmented midbrain tectum. Case report. J Neurosurg 47:605–608
8. Campbell S, Tsannatos C, Pearce JM (1984) The prenatal diagnosis of Joubert's syndrome of familial agenesis of the cerebellar vermis. Prenat Diagn 4:391–395

9. Caspary T, Larkins CE, Anderson KV (2007) The graded response to sonic hedgehog depends on cilia architecture. Develop Cell 12:767–778
10. Chizhikov VV, Davenport J, Zhang Q et al (2007) Cilia proteins control cerebellar morphogenesis by promoting expansion of the granule progenitor pool. J Neurosci 27:9780–9789
11. Coene KL, Roepman R, Doherty D, Afroze B, Kroes HY, Letteboer SJ, Ngu LH, Budny B, van Wijk E, Gorden NT, Azhimi M, Thauvin-Robinet C, Veltman JA, Boink M, Kleefstra T, Cremers FP, van Bokhoven H, de Brouwer AP (2009) OFD1 is mutated in X-linked Joubert syndrome and interacts with LCA5-encoded lebercilin. Am J Hum Genet 85:465–481
12. Dafinger C, Liebau MC, Elsayed SM, Hellenbroich Y, Boltshauser E, Korenke GC, Fabretti F, Janecke AR, Ebermann I, Nürnberg G, Nürnberg P, Zentgraf H, Koerber F, Addicks K, Elsobky E, Benzing T, Schermer B, Bolz HJ (2011) Mutations in KIF7 link Joubert syndrome with Sonic Hedgehog signaling and microtubule dynamics. J Clin Invest 121:2662–2667
13. Dahmane N, Sanchez P, Gitton Y, Palma V, Sun T, Beyna M, Weiner H, Ruiz i Altaba A (2001) The Sonic Hedgehog-Gli pathway regulates dorsal brain growth and tumorigenesis. Development 128:5201–5212
14. Delous M, Baala L, Salomon R, Laclef C, Vierkotten J, Tory K, Golzio C, Lacoste T, Besse L, Ozilou C, Moutkine I, Hellman NE, Anselme I, Silbermann F, Vesque C, Gerhardt C, Rattenberry E, Wolf MT, Gubler MC, Martinovic J, Encha-Razavi F, Boddaert N, Gonzales M, Macher MA, Nivet H, Champion G, Bertheleme JP, Niaudet P, McDonald F, Hildebrandt F, Johnson CA, Vekemans M, Antignac C, Ruther U, Schneider-Maunoury S, Attie-Bitach T, Saunier S (2007) The ciliary gene RPGRIP1L is mutated in cerebello-oculo-renal syndrome (Joubert syndrome type B) and Meckel syndrome. Nat Genet 39:875–881
15. Dixon-Salazar T, Silhavy JL, Marsh SE et al (2004) Mutations in the AHI1 gene, encoding Jouberin, cause Joubert syndrome with cortical polymicrogyria. Am J Hum Genet 75:979–987
16. Doherty D (2009) Joubert syndrome: insights into brain development, cilium biology, and complex disease. Semin Pediatr Neurol 16:143–154
17. Doherty D, Glass IA, Siebert JR, Strouse PJ, Parisi MA, Shaw DW, Chance PF, Barr M Jr, Nyberg D (2005) Prenatal diagnosis in pregnancies at risk for Joubert syndrome by ultrasound and MRI. Prenat Diagn 25:442–447
18. Doherty D, Parisi MA, Finn LS, Gunay-Aygun M, Al-Mateen M, Bates D, Clericuzio C, Demir H, Dorschner M, van Essen AJ, Gahl WA, Gentile M, Gorden NT, Hikida A, Knutzen D, Ozyurek H, Phelps I, Rosenthal P, Verloes A, Weigand H, Chance PF, Dobyns WB, Glass IA (2010) Mutations in 3 genes (*MKS3*, *CC2D2A* and *RPGRIP1L*) cause COACH syndrome (Joubert syndrome with congenital hepatic fibrosis). J Med Genet 47:8–21
19. Eggenschwiler JT, Anderson KV (2007) Cilia and developmental signaling. Annu Rev Cell Dev Biol 23:345–373
20. Exome Variant Server (2011) NHLBI Exome Sequencing Project (ESP), Seattle, WA. URL: http://snp.gs.washington.edu/EVS/. Accessed Sept. 2011
21. Ferrante MI, Zullo A, Barra A, Bimonte S, Messaddeq N, Studer M, Dolle P, Franco B (2006) Oral-facial-digital type I protein is required for primary cilia formation and left–right axis specification. Nat Genet 38:112–117
22. Fluss J, Blaser S, Chitayat D, Akoury H, Glanc P, Skidmore M, Raybaud C (2006) Molar tooth sign in fetal brain magnetic resonance imaging leading to the prenatal diagnosis of Joubert syndrome and related disorders. J Child Neurol 21:320–324
23. Friede RL, Boltshauser E (1978) Uncommon syndromes of cerebellar vermis aplasia. I: Joubert syndrome. Dev Med Child Neurol 20:758–763
24. Garcia-Gonzalo FR, Corbit KC, Sirerol-Piquer MS, Ramaswami G, Otto EA, Noriega TR, Seol AD, Robinson JF, Bennett CL, Josifova DJ, García-Verdugo JM, Katsanis N, Hildebrandt F, Reiter JF (2011) A transition zone complex regulates mammalian ciliogenesis and ciliary membrane composition. Nat Genet 43:776–784
25. Giordano L, Vignoli A, Pinelli L, Brancati F, Accorsi P, Faravelli F, Gasparotti R, Granata T, Giaccone G, Inverardi F, Frassoni C, Dallapiccola B, Valente EM, Spreafico R (2009) Joubert syndrome with bilateral polymicrogyria: clinical and neuropathological findings in two brothers. Am J Med Genet A 149A:1511–1515
26. Gorden NT, Arts HH, Parisi MA, Coene KL, Letteboer SJ, van Beersum SE, Mans DA, Hikida A, Eckert M, Knutzen D, Alswaid AF, Ozyurek H, Dibooglu S, Otto EA, Liu Y, Davis EE, Hutter CM, Bammler TK, Farin FM, Dorschner M, Topcu M, Zackai EH, Rosenthal P, Owens KN, Katsanis N, Vincent JB, Hildebrandt F, Rubel EW, Raible DW, Knoers NV, Chance PF, Roepman R, Moens CB, Glass IA, Doherty D (2008) CC2D2A is mutated in Joubert syndrome and interacts with the ciliopathy-associated basal body protein CEP290. Am J Hum Genet 83:559–571
27. Goodship J, Platt J, Smith R et al (1991) A male with type I orofaciodigital syndrome. J Med Genet 28:691–694
28. Harting I, Kotzaeridou U, Poretti A, Seitz A, Pietz J, Bendszus M, Boltshauser E (2011) Interpeduncular heterotopia in Joubert syndrome: a previously undescribed MR finding. AJNR Am J Neuroradiol 32:1286–1289
29. Han YG, Spassky N, Romaguera-Ros M et al (2008) Hedgehog signaling and primary cilia are required for the formation of adult neural stem cells. Nat Neurosci 11:277–284
30. Heninger E, Otto E, Imm A, Caridi G, Hildebrandt F (2001) Improved strategy for molecular genetic diagnostics in juvenile nephronophthisis. Am J Kidney Dis 37:1131–1139
31. Ishikawa T, Zhu BL, Li DR, Zhao D, Michiue T, Maeda H (2008) An autopsy case of an infant with Joubert syndrome who died unexpectedly and a review of the literature. Forensic Sci Int 179:e67–e73
32. Ivarsson SA, Bjerre I, Brun A, Ljungberg O, Maly E, Taylor I (1993) Joubert syndrome associated with Leber amaurosis and multicystic kidneys. Am J Med Genet 45:542–547
33. Joubert M, Eisenring JJ, Robb JP, Andermann F (1969) Familial agenesis of the cerebellar vermis. A syndrome of episodic hyperpnea, abnormal eye movements, ataxia, and retardation. Neurology 19:813–825
34. Koirala S, Jin Z, Piao X, Corfas G (2009) GPR56-regulated granule cell adhesion is essential for rostral cerebellar development. J Neurosci 29:7439–7449
35. Kumandas S, Akcakus M, Coskun A, Gumus H (2004) Joubert syndrome: review and report of seven new cases. Eur J Neurol 11:505–510
36. Lancaster MA, Gopal DJ, Kim J, Saleem SN, Silhavy JL, Louie CM, Thacker BE, Williams Y, Zaki MS, Gleeson JG (2011) Defective Wnt-dependent cerebellar midline fusion in a mouse model of Joubert syndrome. Nat Med 17:726–731
37. Liu JS (2011) Molecular genetics of neuronal migration disorders. Curr Neurol Neurosci Rep 11(2):171–178
38. Lopes CA, Prosser SL, Romio L, Hirst RA, O'Callaghan C, Woolf AS, Fry AM (2011) Centriolar satellites are assembly points for proteins implicated in human ciliopathies, including oral-facial-digital syndrome 1. J Cell Sci 124:600–612
39. Maria BL, Quisling RG, Rosainz LC, Yachnis AT, Gitten J, Dede D, Fennell E (1999) Molar tooth sign in Joubert syndrome: clinical, radiologic, and pathologic significance. J Child Neurol 14:368–376
40. McGraw P (2003) The molar tooth sign. Radiology 229:671–672

41. Millen KJ, Gleeson JG (2008) Cerebellar development and disease. Curr Opin Neurobiol 18:12–19
42. Ocbina PJR, Anderson KV (2008) Intraflagellar transport, cilia and mammalian Hedgehog signaling: analysis in mouse embryonic fibroblasts. Dev Dyn 237:2030–2038
43. Padgett KR, Maria BL, Yachnis AT, Blackband SJ (2002) Ex vivo high-resolution magnetic resonance imaging of the brain in Joubert's syndrome. J Child Neurol 17:911–913
44. Parisi MA, Dobyns WB (2003) Human malformations of the midbrain and hindbrain: review and proposed classification scheme. Mol Genet Metab 80:36–53
45. Parisi MA, Doherty D, Chance PF, Glass IA (2007) Joubert syndrome (and related disorders) (OMIM 213300). Eur J Hum Genet 15:511–521
46. Poretti A, Brehmer U, Scheer I et al (2008) Prenatal and neonatal MR imaging findings in oral-facial-digital syndrome type VI. AJNR 29:1090–1091
47. Poretti A, Huisman TA, Scheer I, Boltshauser E (2011) Joubert syndrome and related disorders: spectrum of neuroimaging findings in 75 patients. AJNR Am J Neuroradiol 32:1459–1463
48. Prattichizzo C, Macca M, Novelli V, Giorgio G, Barra A, Franco B, Oral-Facial-Digital Type ICG (2008) Mutational spectrum of the oral-facial-digital type I syndrome: a study on a large collection of patients. Hum Mutat 29:1237–1246
49. Putoux A, Thomas S, Coene KL, Davis EE, Alanay Y, Ogur G, Uz E, Buzas D, Gomes C, Patrier S, Bennett CL, Elkhartoufi N, Frison MH, Rigonnot L, Joyé N, Pruvost S, Utine GE, Boduroglu K, Nitschke P, Fertitta L, Thauvin-Robinet C, Munnich A, Cormier-Daire V, Hennekam R, Colin E, Akarsu NA, Bole-Feysot C, Cagnard N, Schmitt A, Goudin N, Lyonnet S, Encha-Razavi F, Siffroi JP, Winey M, Katsanis N, Gonzales M, Vekemans M, Beales PL, Attié-Bitach T (2011) KIF7 mutations cause fetal hydrolethalus and acrocallosal syndromes. Nat Genet 43:601–606
50. Quisling RG, Barkovich AJ, Maria BL (1999) Magnetic resonance imaging features and classification of central nervous system malformations in Joubert syndrome. J Child Neurol 14:628–635 (discussion 669–672)
51. Ribes V, Stutzmann F, Bianchetti L, Guillemot F, Dolle P, Le Roux I (2008) Combinatorial signaling controls Neurogenin2 expression at the onset of spinal neurogenesis. Dev Biol 321:470–481
52. Romano S, Boddaert N, Desguerre I, Hubert L, Salomon R, Seidenwurm D, Bahi-Buisson N, Nabbout R, Sonigo P, Lyonnet S, Brunelle F, Munnich A, de Lonlay P (2006) Molar tooth sign and superior vermian dysplasia: a radiological, clinical, and genetic study. Neuropediatrics 37:42–45
53. Saleem SN, Zaki MS (2010) Role of MR imaging in prenatal diagnosis of pregnancies at risk for Joubert syndrome and related cerebellar disorders. AJNR Am J Neuroradiol 31:424–429
54. Saleem SN, Zaki MS, Soliman NA, Momtaz M (2011) Prenatal magnetic resonance imaging diagnosis of molar tooth sign at 17 to 18 weeks of gestation in two fetuses at risk for Joubert syndrome and related cerebellar disorders. Neuropediatrics 42:35–38
55. Sang L, Miller JJ, Corbit KC, Giles RH, Brauer MJ, Otto EA, Baye LM, Wen X, Scales SJ, Kwong M, Huntzicker EG, Sfakianos MK, Sandoval W, Bazan JF, Kulkarni P, Garcia-Gonzalo FR, Seol AD, O'Toole JF, Held S, Reutter HM, Lane WS, Rafiq MA, Noor A, Ansar M, Devi AR, Sheffield VC, Slusarski DC, Vincent JB, Doherty DA, Hildebrandt F, Reiter JF, Jackson PK (2011) Mapping the NPHP–JBTS–MKS protein network reveals ciliopathy disease genes and pathways. Cell 145:513–528
56. Saraiva JM, Baraitser M (1992) Joubert syndrome: a review. Am J Med Genet 43:726–731
57. Sattar S, Gleeson JG (2011) The ciliopathies in neuronal development: a clinical approach to investigation of Joubert syndrome and Joubert syndrome-related disorders. Dev Med Child Neurol 53:793–798
58. Sawamoto K, Wichterie H, Gonzalez-Perez O et al (2006) New neurons follow the flow of cerebrospinal fluid in the adult brain. Science 311:629–632
59. Schneider L, Cammer M, Lehman J et al (2010) Directional cell migration and chemotaxis in wound healing response to PDGF-AA are coordinated by the primary cilium in fibroblasts. Cell Physiol Biochem 25:279–292
60. Senocak EU, Oguz KK, Haliloglu G, Topcu M, Cila A (2010) Structural abnormalities of the brain other than molar tooth sign in Joubert syndrome-related disorders. Diagn Interv Radiol 16:3–6
61. Singla V, Romaguera-Ros M, Garcia-Verdugo JM, Reiter JF (2010) Ofd1, a human disease gene, regulates the length and distal structure of centrioles. Dev Cell 18:410–424
62. Spassky N, Han YG, Aguilar A, Strehl L, Besse L, Laclef C, Ros MR, Garcia-Verdugo JM, Alvarez-Buylla A (2008) Primary cilia are required for cerebellar development and Shh-dependent expansion of progenitor pool. Dev Biol 317:246–259
63. Sztriha L, Al-Gazali LI, Aithala GR, Nork M (1999) Joubert's syndrome: new cases and review of clinicopathologic correlation. Pediatr Neurol 20:274–281
64. ten Donkelaar HJ, Hoevenaars F, Wesseling P (2000) A case of Joubert's syndrome with extensive cerebral malformations. Clin Neuropathol 19:85–93
65. ten Donkelaar HJ, Lammens M (2009) Development of the human cerebellum and its disorders. Clin Perinatol 36:513–530
66. Valente EM, Logan CV, Mougou-Zerelli S, Lee JH, Silhavy JL, Brancati F, Iannicelli M, Travaglini L, Romani S, Illi B, Adams M, Szymanska K, Mazzotta A, Lee JE, Tolentino JC, Swistun D, Salpietro CD, Fede C, Gabriel S, Russ C, Cibulskis K, Sougnez C, Hildebrandt F, Otto EA, Held S, Diplas BH, Davis EE, Mikula M, Strom CM, Ben-Zeev B, Lev D, Sagie TL, Michelson M, Yaron Y, Krause A, Boltshauser E, Elkhartoufi N, Roume J, Shalev S, Munnich A, Saunier S, Inglehearn C, Saad A, Alkindy A, Thomas S, Vekemans M, Dallapiccola B, Katsanis N, Johnson CA, Attie-Bitach T, Gleeson JG (2010) Mutations in *TMEM216* perturb ciliogenesis and cause Joubert, Meckel and related syndromes. Nat Genet 42:619–625
67. van Dorp DB, Palan A, Kwee ML, Barth PG, van der Harten JJ (1991) Joubert syndrome: a clinical and pathological description of an affected male and a female fetus from the same sibship. Am J Med Genet 40:100–104
68. Watanabe H, Murakami F (2009) Real time analysis of pontine neurons during initial stages of nucleogenesis. Neurosci Res 64:20–29
69. Yachnis AT, Rorke LB (1999) Neuropathology of Joubert syndrome. J Child Neurol 14:655–659 (discussion 669–672)
70. Yu W, McDonnell K, Taketo MM, Bai CB (2008) Wnt signaling determines ventral spinal cord cell fates in a time-dependent manner. Development 135:3687–3696